Cap-poly(A) synergy in mammalian cell-free extracts. Investigation of the requirements for poly(A)-mediated stimulation of translation initiation

Yanne M. Michel, Didier Poncet, Maria Piron, Katherine M. Kean, Andrew M. Borman

THE JOURNAL OF BIOLOGICAL CHEMISTRY
Vol. 275, No. 41, Issue of October 13, pp. 32268–32276, 2000

Printed in U.S.A.

Cap-Poly(A) Synergy in Mammalian Cell-free Extracts

INVESTIGATION OF THE REQUIREMENTS FOR POLY(A)-MEDIATED STIMULATION OF TRANSLATION INITIATION*

Received for publication, May 19, 2000, and in revised form, July 25, 2000
Published, JBC Papers in Press, August 1, 2000, DOI 10.1074/jbc.M004304200

Yanne M. Michel, Didier Poncet‡, Maria Piron‡§, Katherine M. Kean¶, and Andrew M. Borman

From the Unité de Génétique Moléculaire des Virus Respiratoires, CNRS URA 1966, Institut Pasteur, 25 rue du Dr. Roux, 75724 Paris Cedex 15 and the ‡Laboratoire de Virologie et Immunologie Moléculaires INRA, CRJJ, Domaine de Vilvert, 78352 Jouy-en-Josas Cedex, France

The 5′ cap and 3′ poly(A) tail of eukaryotic mRNAs cooperate to stimulate synergistically translation initiation *in vivo*, a phenomenon observed to date *in vitro* only in translation systems containing endogenous competitor mRNAs. Here we describe nuclease-treated rabbit reticulocyte lysates and HeLa cell cytoplasmic extracts that reproduce cap-poly(A) synergy in the absence of such competitor RNAs. Extracts were rendered poly(A)-dependent by ultracentrifugation to partially deplete them of ribosomes and associated initiation factors. Under optimal conditions, values for synergy in reticulocyte lysates approached 10-fold. By using this system, we investigated the molecular mechanism of poly(A) stimulation of translation. Maximal cap-poly(A) cooperativity required the integrity of the eukaryotic initiation factor 4G-poly(A)-binding protein (eIF4G-PABP) interaction, suggesting that synergy results from mRNA circularization. In addition, polyadenylation stimulated uncapped cellular mRNA translation and that driven by the encephalomyocarditis virus internal ribosome entry segment (IRES). These effects of poly(A) were also sensitive to disruption of the eIF4G-PABP interaction, suggesting that 5′–3′ end cross-talk is functionally conserved between classical mRNAs and an IRES-containing mRNA. Finally, we demonstrate that a rotaviral non-structural protein that evicts PABP from eIF4G is capable of provoking the shut-off of host cell translation seen during rotavirus infection.

The 5′ ends of all eukaryotic mRNAs are modified post-transcriptionally to carry a methylated cap structure, m^7GpppN (1). Aside from roles in RNA splicing, stabilization, and transport, the cap structure significantly enhances the recruitment of the 40 S ribosomal subunit to the mRNA 5′ end during translation initiation. The latter function requires recognition of the cap by the eukaryotic initiation factor (eIF)[1] 4F. The eIF4F holoenzyme complex consists of the cap-binding protein eIF4E and an ATP-dependent RNA helicase (eIF4A) bound toward the N- and C-terminal ends, respectively, of a scaffold molecule eIF4G (for review see Ref. 2). The C-terminal domain of eIF4G also interacts with eIF3, a complex that associates directly with the 40 S ribosomal subunit.

Most mRNAs carry a poly(A) tail at their 3′ ends, which determines mRNA stability (for review see Ref. 3) and enhances translation initiation efficiency (4). However, reports concerning the actual extent of enhancement of translation initiation by the poly(A) tail are somewhat contradictory, depending on the system used. Moderate poly(A)-mediated stimulation of translation can occur in the absence of a cap structure or functional eIF4E, but a cap is absolutely required for optimal poly(A)-mediated translation stimulation (5, 6). Studies performed in the rabbit reticulocyte lysate (RRL) and other nuclease-treated cell-free extracts demonstrated that the stimulation of translation upon capping and poly(A) tailing were additive phenomena (7, 8). In contrast, *in vivo* translation studies have demonstrated that the poly(A) tail and cap interact synergistically to stimulate translation initiation in yeast, plant spheroplasts, and mammalian cells (5, 6, 9). Synergy between the cap and poly(A) tail in promoting translation has also been observed in non-nucleased yeast and *Drosophila* cell-free translation extracts (6, 8, 10). However, synergy was abrogated by disruption of endogenous mRNA translation in yeast cells (9) or by nuclease treatment of yeast cell-free extracts unless such extracts were supplemented with excess competitor mRNAs (6). It was thus suggested that an RNA requires the poly(A) tail for translation only when it is competing with other capped and polyadenylated RNAs for limiting concentrations of ribosomes or translation factors. Support for this suggestion came from the demonstration that mutations that affect polyadenylation only significantly reduce translation when introduced into yeast strains harboring low concentrations of ribosomal subunits (11).

Biochemical analyses clearly demonstrated that poly(A) tail-mediated translation stimulation involves increased 40 S subunit recruitment to mRNAs and requires the intervention of poly(A) tail-binding protein (PABP) (5). PABP was recently demonstrated to interact physically with the N-terminal region of eIF4G from yeast (12) and from mammals (13). Thus, a closed loop model of translation initiation on capped, polyadenylated mRNAs was postulated (3). Formal proof of mRNA circularization via the cap-eIF4E-eIF4G-PABP-poly(A) interaction was provided by atomic force microscopy of mRNAs complexed with purified recombinant proteins (14). However, the functional consequences of mRNA circularization have not been directly addressed experimentally.

Since the closed loop model of translation initiation depends

* This work was supported in part by a grant from the Program de Recherches Fondamentales en Microbiologie, Maladies Infectieuses et Parasitologie from the MENRT (to D. P.). The costs of publication of this article were defrayed in part by the payment of page charges. This article must therefore be hereby marked "*advertisement*" in accordance with 18 U.S.C. Section 1734 solely to indicate this fact.

§ Present address: Dept. Medecine Interne-Hepatology, Vall D'Hebron Hospital, 08035 Barcelona, Spain.

¶ To whom correspondence should be addressed. Tel.: 33 1 40 61 33 55; Fax: 33 1 40 61 30 45; E-mail: kathiemb@pasteur.fr.

[1] The abbreviations used are: eIF, eukaryotic initiation factor; PABP, poly(A)-binding protein; IRES, internal ribosome entry segment; UTR, untranslated region; HIV-I, human immunodeficiency virus type I; nt, nucleotide; PCR, polymerase chain reaction; NSP, non-structural protein; NS, non-structural; EMCV, encephalomyocarditis virus.

upon interactions between the 5′-terminal cap structure and the 3′ poly(A) tail, the subset of eukaryotic and viral mRNAs that are either uncapped or non-polyadenylated are difficult to accommodate within this model. For certain viral mRNAs, an alternative means of closing the loop has already been proposed. For instance, for capped, non-polyadenylated rotaviral mRNAs, the viral non-structural protein NSP3 binds the conserved rotaviral RNA 3′ end and can interact with eIF4G and displace PABP from the eIF4F complex (15, 16). However, the case for picornaviral RNAs remains unresolved. Whereas these viral RNAs are polyadenylated, they are uncapped, and translation initiation is independent of the RNA 5′ end. In fact, ribosome entry on these RNAs occurs internally, several hundred nucleotides downstream of the 5′ end, and is driven by a complex RNA signal of some 400–500 nt, coined the IRES (internal ribosome entry segment) (for review see Ref. 17).

Here, we describe mammalian cell-free translation systems that exhibit cap-poly(A) synergy in the absence of added competitor mRNAs. These systems, derived from extracts in which IRES-driven translation is routinely studied, were used to examine the molecular mechanism of poly(A) tail-mediated translational stimulation on classical eukaryotic mRNAs and on an mRNA harboring an IRES.

EXPERIMENTAL PROCEDURES

Plasmid Constructions—Plasmids were derived from the previously described pXLJCon clone (18), which contains the cDNA for *Xenopus laevis* cyclin B2 (including the 5′ and 3′-UTRs) under the control of the bacteriophage T7 promoter, followed by a short artificial polylinker and then the cDNA corresponding to a truncated coding region and the 3′-UTR of the influenza virus NS protein. For the present study, the NS-coding region of pXLJCon was replaced by the gene encoding the p24 capsid protein of human immunodeficiency virus type I (HIV-I_{LAI}; see Ref. 19). The different resulting constructs are represented schematically in Fig. 1. In a first step, the NS-coding region and 3′-UTR were excised by digestion with *Bam*HI and *Eco*RI and replaced by a PCR-generated fragment corresponding to the 150-nt NS 3′-UTR (sense primer, 5′ ATGGATCCCGGGTGAAGAAGTGAGACACAAAC 3′; antisense primer SP6 primer; 30 cycles: 96 °C 30 s, 55 °C 45 s, 72 °C 1 min) to generate pXLinker. In a second step, a PCR fragment containing the entire p24-coding region was generated to contain unique *Nco*I and *Sma*I restriction sites at the 5′ and 3′ ends, respectively (PCR primers p24sense 5′ CCATGGATCCTATAGTGCAGAACATA 3′ and p24antisense 5′ TCCCCCGGGCAAAACTCTTGCCTTATG 3′; 30 cycles: 96 °C 30 s, 55 °C 45 s, 72 °C 2 min). Introduction of the *Nco*I-*Sma*I-digested PCR product into pXLinker digested with the same enzymes results in the fusion of p24 in frame between the polylinker ATG initiation codon and the TGA stop codon that precedes the NS 3′-UTR, producing pB2Op24. The resulting p24 gene product thus carries 2 amino acid extensions at each of the N and C termini. For the construction of pB2ΔIRESp24, nucleotides 10–547 of the human rhinovirus type 2 5′-UTR were excised from the previously described pXLJ10–547 (18) by digestion with *Sal*I and *Bam*HI and were inserted into pB20p24 digested with the same enzymes. The monocistronic p0p24 plasmid was constructed by replacing the small *Sal*I-*Eco*RI fragment of pJCon (18) with that from pB20p24. To insert the entire EMCV IRES (from the poly(C) tract to nt 848) into p0p24 (to produce pEMCVp24), the in-filled *Eco*RI-*Nco*I small fragment from p-CITE (Novagen) was inserted into the in-filled *Bam*HI site of p0p24.

To produce a plasmid encoding only cyclin B2, and with 5′- and 3′-UTRs identical to those in pB20p24, the full 5′-UTR and cyclin B2-coding region up to the stop codon was amplified by PCR so as to contain a unique *Sma*I site at its 3′ end (sense primer T7 promoter, antisense primer 5′ TCTTCACCCGGGAGAGAGACTTGCAGCAAG 3′; 30 cycles: 96 °C 30 s, 55 °C 45 s, 72 °C 2 min). The A*sp*718I-S*ma*I internal fragment of this PCR product that includes the 3′ end of the coding region was then used to replace the full *Asp*718-*Sma*I region of the pB20p24 construct. The resulting pB2 construct thus contains the cyclin-coding region, with a 2-amino acid C-terminal extension, fused in frame with the NS stop codon and 3′-UTR (Fig. 1).

Versions of all of these constructions carrying poly(A) stretches were constructed by inserting annealed 5′ $AATTA_{50}G$ 3′ and 5′ $AATTCT_{50}$ 3′ oligonucleotides into the unique *Eco*RI site at the 3′ end of the NS 3′-UTR. This gives an A_{50} followed directly by a unique *Eco*RI site, 24 nt downstream of the authentic polyadenylation signal. Constructs were verified by automatic sequencing.

Antibodies and Recombinant Proteins—Human rhinovirus 2A proteinase, expressed in *Escherichia coli* and purified exactly as described previously (20), was a gift from T. Skern. A recombinant fragment of rotavirus NSP3 protein encompassing amino acids 163–313 was overexpressed in *E. coli* and purified exactly as described previously (16, 21). Both NSP3 and 2A proteinase were dialyzed against H100 buffer (10 mM HEPES-KOH, pH 7.5, 100 mM KCl, 1 mM $MgCl_2$, 0.1 mM EDTA, and 7 mM β-mercaptoethanol) prior to use. Rabbit anti-eIF4G peptide 7 antiserum (raised against residues 327–342) was a gift of R. Rhoads. Monoclonal antibody 10E10 against human PABP was a gift of M. Görlach.

Preparation of Translation Extracts—Nuclease-treated RRL was partially depleted of ribosomes by ultracentrifugation. Briefly, 2-ml volumes of flexi-reticulocyte lysate (Promega) were centrifuged at 90,000 rpm for 15–20 min in a Beckman TL-100 benchtop ultracentrifuge. The supernatant was removed, aliquoted, and stored at −80 °C. The ribosomal pellets were resuspended in 1/10 volume (with respect to the initial volume of lysate) of H100 buffer and frozen at −80 °C. Non-nuclease HeLa cell S10 extracts were prepared exactly as described previously (22) and were dialyzed overnight against H100 buffer. Translation-competent HeLa cell S10 extracts were prepared and treated with micrococcal nuclease as described (23) except that dialysis was performed against H100 buffer. Ribosome depletion of translation-competent HeLa cell S10 extracts was performed as described above for RRL.

In Vitro Transcriptions and Translations—In vitro transcriptions and translations were performed as described previously (24) except that artificially capped transcripts were synthesized in the presence of 0.8 mM cap analogue (Ambion Inc.). Transcription reactions included trace quantities of [α-^{32}P]UTP to allow accurate quantification of RNA yields. All RNAs were purified on G-50 Sephadex spin columns (Roche Molecular Biochemicals) to eliminate non-incorporated cap analogue and nucleotides prior to ethanol precipitation and washing with 70% ethanol.

In vitro translation reactions were performed in the presence of [^{35}S]methionine. RRL-based reactions contained 50% by volume of flexi-reticulocyte lysate (Promega) or ribosome-depleted RRL and 33% by volume of H100 buffer or non-nucleased HeLa cell S10 extract in H100 buffer, and were programmed with the indicated concentrations of *in vitro* transcribed mRNAs. Final concentrations, respectively, of added KCl and $MgCl_2$ were 102 and 0.8 mM (for the experiments presented in Fig. 2) and 115 and 0.9 mM in all subsequent reactions. For translation reactions performed in translation-competent HeLa cell extracts, reactions containing 40% of HeLa cell extract were programmed with 6.5 μg/ml of *in vitro* transcribed mRNAs. In certain experiments, translation reactions were supplemented with ribosomal pellet resuspended in H100 buffer, or purified recombinant proteins (2A proteinase or a fragment of NSP3) also in H100 buffer.

Translations were performed for 90 min at 30 °C, and the translation products were analyzed by SDS-polyacrylamide gel electrophoresis as described previously (25), using gels containing 20% w/v acrylamide. Dried gels were exposed to Hyperfilm β-max (Amersham Pharmacia Biotech) typically for 12–16 h. Densitometric quantification of translation products was as described previously (24) using multiple exposures of each gel to ensure that the linear response range of the film was respected and that low levels of translation could be accurately quantified. In some experiments, the total radioactivity incorporated into proteins was assayed by trichloroacetic acid precipitation exactly as described (26). The data presented in each figure are representative of at least three independent translation assays.

Sucrose Gradient Analysis of Ribosome Profiles—Quantification of 40 S and 60 S ribosomal subunits in translation extracts was performed exactly as described previously (27), using 110-μl aliquots of RRL or translation-competent HeLa cell S10 extract (20–30 A_{260} units).

Co-immunoprecipitation and Western Blotting—Translation reactions (200 μl) were incubated with and without recombinant NSP3 for 30 min at 30 °C before immunoprecipitation as described previously (16) with 1 μl per reaction of rabbit anti-eIF4G peptide 7 antisera. Western blot analysis of immunoprecipitated proteins was exactly as described (24). Membranes were incubated with mouse anti-PABP primary antibody, followed by horseradish peroxidase-linked goat anti-mouse secondary antibodies, and were revealed by enhanced chemiluminescence (ECLplus, Amersham Pharmacia Biotech).

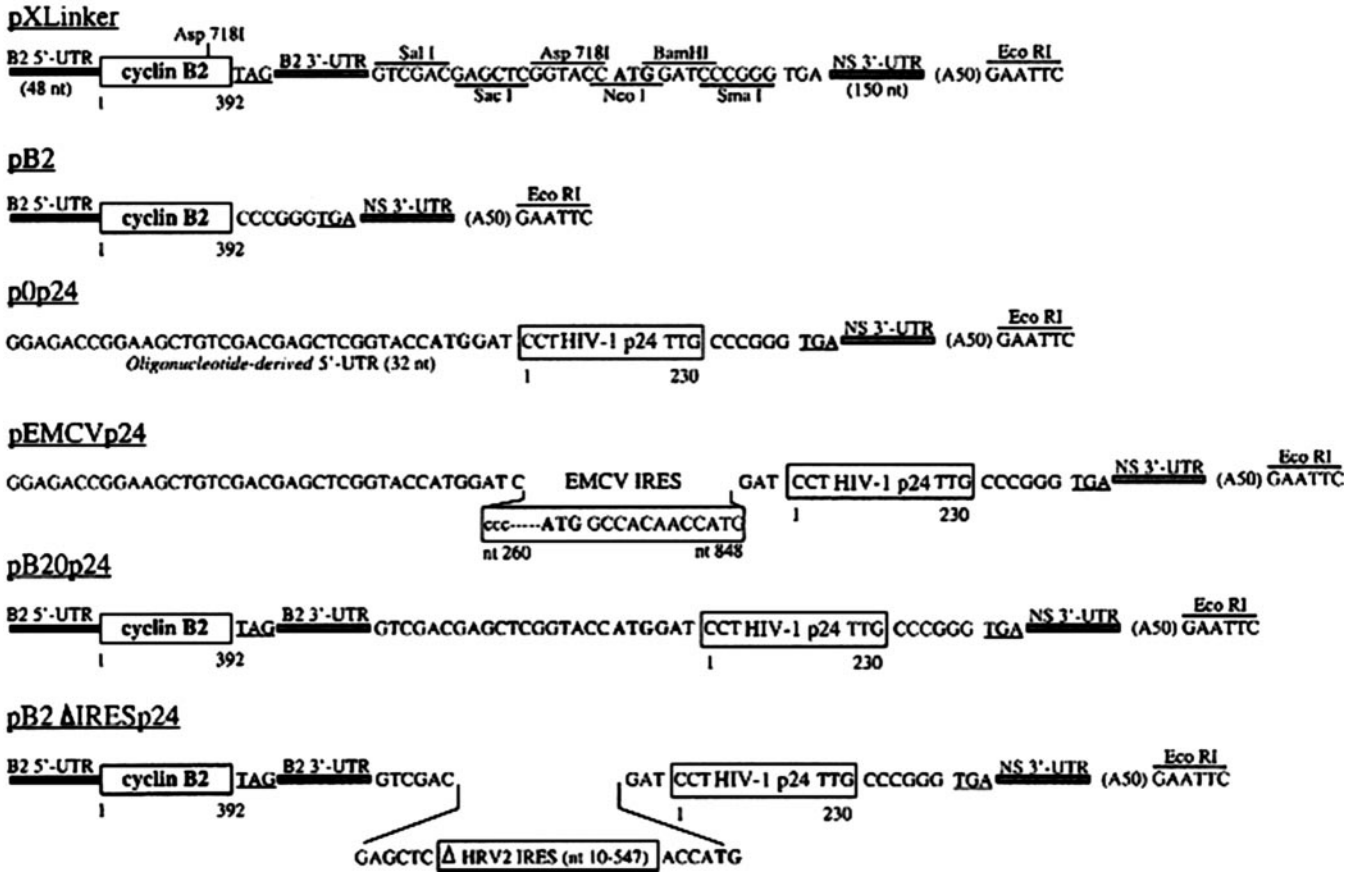

FIG. 1. **Schematic representation of plasmids used in this work.** The *X. laevis* cyclin B2 and HIV-I p24-coding regions and the regions corresponding to the active EMCV and inactive HRV2 IRESes are shown as *open boxes. Numbers* below coding regions refer to the first and last amino acids of each reporter gene product; for the HRV2 and EMCV IRESes, the numbering is based on the viral genome sequence and denotes the first and last nucleotides of viral sequence. Other 5′- and 3′-UTRs are depicted as *thick lines*; the ATG codon that serves to initiate HIV-I p24 synthesis is shown in *bold*; restriction sites and stop codons are *underlined.* Clones were constructed in duplicate, differing only in the presence or absence of anA_{50} insertion (*bracketed*) at the *Eco*RI site used for linearization prior to transcription.

RESULTS

To date, several cell-free translation extracts have been described that reproduce the cap-poly(A) synergistic stimulation of translation previously observed *in vivo* (6, 8, 10). However, synergy was only observed in these cell-free extracts in the presence of competitor mRNAs (6), which complicates a dissection of the molecular basis of synergy. The primary aim of the study presented here was to develop cell-free extracts from mammals that would exhibit synergy between the cap and poly(A) tail in the absence of added competitor mRNAs, and therefore could be used to examine the molecular mechanism of cap-poly(A) cooperativity.

Development of an RRL-based Translation System That Exhibits Cap-Poly(A) Synergy—The effects of the poly(A) tail on translation can be measured in two ways: by comparing the translation efficiency of uncapped mRNAs with and without a poly(A) tail, or by examining the synergy obtained upon addition of both poly(A) and a cap to an mRNA (28). To carry out a comprehensive analysis, we compared the translation efficiency of four versions of a given mRNA as follows: neither capped nor polyadenylated (−/−), capped and non-polyadenylated (+/−), uncapped and polyadenylated (−/+), and both capped and polyadenylated (+/+). These were synthesized *in vitro* from cDNA transcription templates that only differed by an oligonucleotide-derived homopolymer A_{50} insertion preceding a unique *Eco*RI site at the end of a 150-nt 3′-UTR (pB2; see "Experimental Procedures" and Fig. 1). Thus, the polyadenylated mRNAs described here terminate with an A_{50}-GAAUU tail. It has previously been shown that a short 3′ end heterologous sequence does not affect poly(A) tail-promoted translation (6), and that 50 A residues suffice to demonstrate the roles of the poly(A) tail in translation initiation (9, 29).

B2 RNAs were first translated in a nuclease-treated RRL *in vitro* translation system, in the absence of added competitor RNAs (see Fig. 2*A*, RRL + 0% HeLaS10 lanes). As expected, translation of capped B2 mRNA in this system was some 30-fold more efficient than that of the uncapped equivalent (compare +/− and −/− *lanes*). Polyadenylation of uncapped B2 mRNA stimulated its translation approximately 6-fold (compare −/+ and −/− *lanes*). Moreover, additive stimulation of translation was achieved by polyadenylation and capping (compare the +/+ *lane* with the sum of the +/− and −/+ *lanes*), in accordance with previous reports (7, 8). Since poly(A)-mediated synergistic stimulation of translation in nuclease-treated yeast extracts required the presence of competitor RNAs (6), we next measured the translation activity of the B2 mRNAs in RRL supplemented with increasing amounts of non-nucleased HeLa cell S10 extract. Non-nucleased cell extract was employed rather than purified poly(A) RNA to ensure that physiological cell equivalents of mRNA were added. Global translation efficiency was significantly lowered in such conditions (Fig. 2*A*, RRL compare *0, 16.5* and *33 HeLaS10 lanes*). Furthermore, the stimulatory effects of addition of a cap or poly(A) tail alone were then reduced (see values for *Relative Stimulation,* Fig. 2*A*). In contrast, slight cap-poly(A) synergy (calculated as the relative stimulation of +/+ RNA divided by the sum of the relative stimulations of −/+ and +/− RNAs) was reproducibly observed. This increased concomitantly with the quantity of

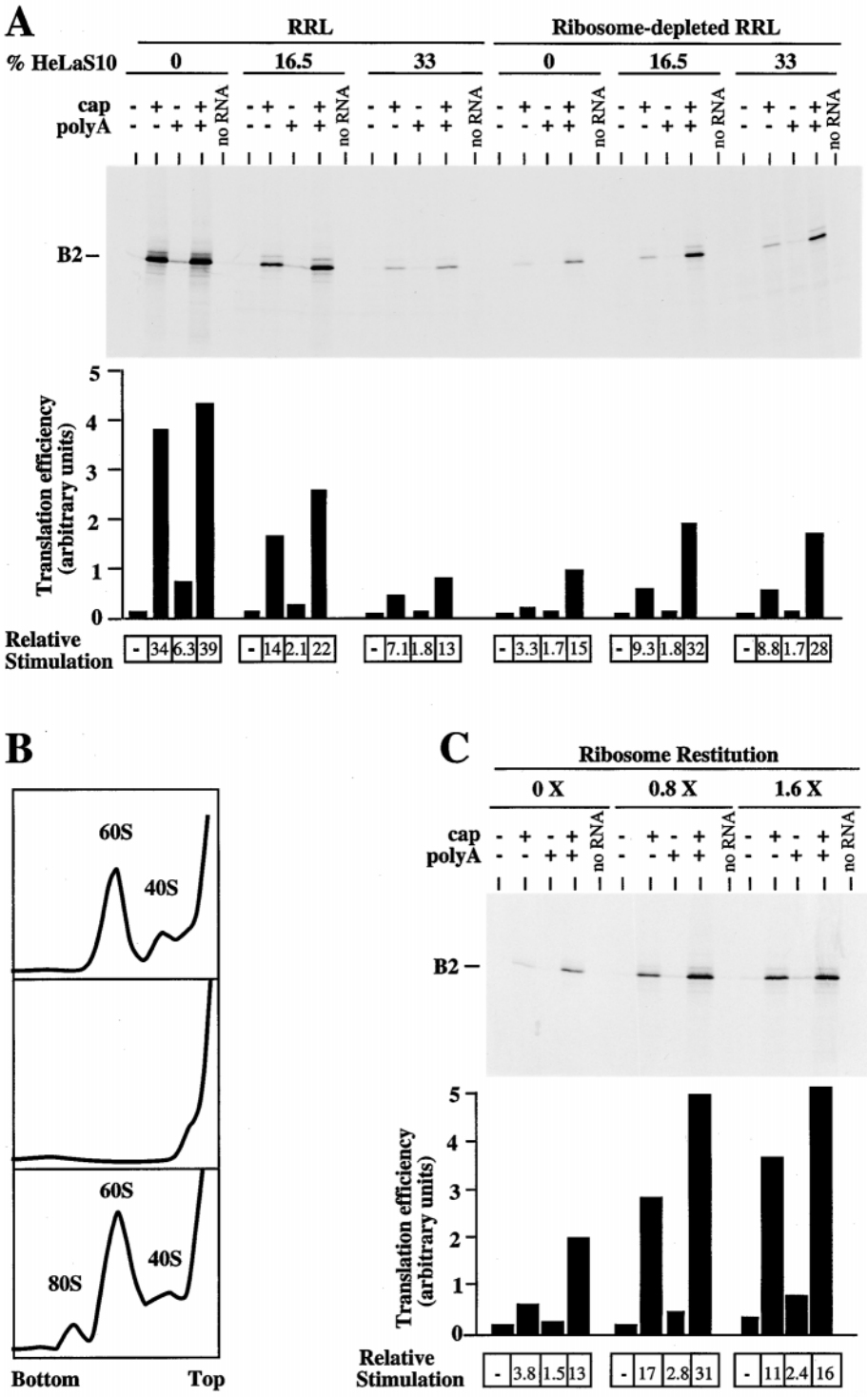

FIG. 2. **Development of an RRL-based translation system that exhibits cap-poly(A) synergy.** *A,* standard RRL or ribosome-depleted RRL were supplemented with 33% (v/v) of non-nucleased HeLa cell S10 extract (*33 lanes*), H100 buffer (*0 lanes*), or 1:1 of S10 extract and H100 buffer (*16.5 lanes*). Reactions were programmed with RNAs (6.5 μg/ml) transcribed *in vitro* from pB2 in four distinct versions as indicated *above* each lane. Control reactions were programmed with water (no RNA lanes). Translations were processed as described under "Experimental Procedures." The autoradiograph of the dried 20% polyacrylamide gel is shown. The position of the cyclin B2 translation product is marked. Translation efficiency derived from densitometric quantification is plotted *below* each lane. Relative stimulation of translation was calculated by comparing the translation efficiency of capped and/or polyadenylated RNA to that of the −/− RNA (arbitrary units for the −/− RNAs from *left to right* of 0.11, 0.12, 0.06, 0.06, 0.05, and 0.07). *B,* sucrose gradient analysis of the proportions of 40 S and 60 S ribosomal subunits in equivalent volumes of standard RRL (*upper plot*), ribosome-depleted RRL (*middle plot*), or RRL supplemented with 33% of non-nucleased HeLa cell S10 extract (*lower plot*). Absorbance at 254 nm (*y* axis) is plotted against gradient fraction number. The positions of the 40 S, 60 S, and 80 S peaks and the top and bottom of the gradients are indicated. *C,* ribosome-depleted RRL supplemented with H100 buffer (*0*×) or ribosomes recovered from RRL after ultracentrifugation (final concentrations of 0.8 or 1.6× with respect to intact RRL; see "Experimental Procedures") and programmed with the indicated versions of B2 RNA as in *A*. The data are presented as in *A*. Arbitrary units for the −/− lanes were 0.16, 0.17, and 0.33.

added competitor but never reached 2-fold.

It has been suggested that the concentration of free ribosomes *per se* determines the magnitude of poly(A)-mediated translation stimulation (11). Thus, in an attempt to amplify cap-poly(A) synergy in the RRL system, and to circumvent the need for addition of competitor RNAs, RRL was partially depleted of ribosomes by ultracentrifugation (see "Experimental Procedures"). Translation efficiency was dramatically reduced in reactions containing the ultracentrifugation supernatant compared with those based on intact RRL (Fig. 2*A*, compare *ribosome-depleted RRL* and *RRL lanes*; *0% HeLaS10*). The stimulatory effects of capping non-polyadenylated mRNA and polyadenylating uncapped mRNA were also reduced as compared with the reactions performed in standard RRL. However, cap-poly(A) cooperative stimulation of translation was observed (synergy of approximately 3-fold). Whereas the addition of a non-nucleased HeLa cell S10 extract to ribosome-depleted RRL moderately improved global translation efficiency, it did not affect the synergy (see Fig. 2*A, right-hand side*), presumably because the positive effects of the added competitor mRNAs in increasing synergy are negated by the free ribosomes and initiation factors present in the HeLa cell extract. Thus, all further studies using the RRL system were performed with ribosome-depleted RRL, without HeLa cell extract supplementation.

Sucrose gradient analysis was performed to determine the

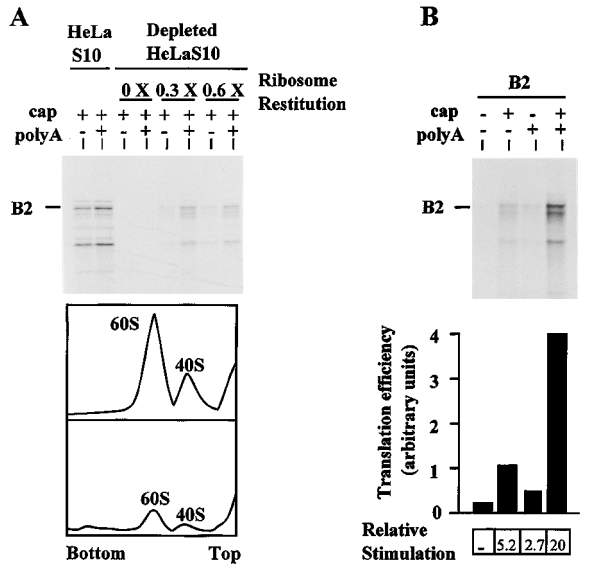

FIG. 3. **Cap-poly(A) synergy in a human cell-free extract.** *A,* nuclease-treated translation-competent HeLa cell S10 extract (*HeLaS10*) or ribosome-depleted HeLa S10 supplemented with either H100 buffer (*0*×) or ribosomes recovered from HeLa cell S10 extract after ultracentrifugation (final concentrations with respect to control HeLa cell S10 extract) were programmed with 6.5 μg/ml capped, B2 RNAs in non-polyadenylated or polyadenylated form (as indicated). Translation products were analyzed as described in the legend to Fig. 2. Sucrose gradient analysis of the proportions of 40 S and 60 S ribosomal subunits in equivalent volumes of nuclease-treated translation-competent HeLa cell S10 extract (*upper plot*), or ribosome-depleted HeLa S10 supplemented with ribosomes recovered from the centrifugation pellet (final concentration of 0.3× with respect to intact HeLa cell S10 extract; *lower plot*) was performed as described under "Experimental Procedures." Data are presented as in Fig. 2. *B,* ribosome-depleted HeLa S10 supplemented with 0.3× ribosomes was programmed with 6.5 μg/ml of the various *in vitro* transcribed B2 mRNAs as shown *above* each lane. Translation products were analyzed as described in the legend to Fig. 2.

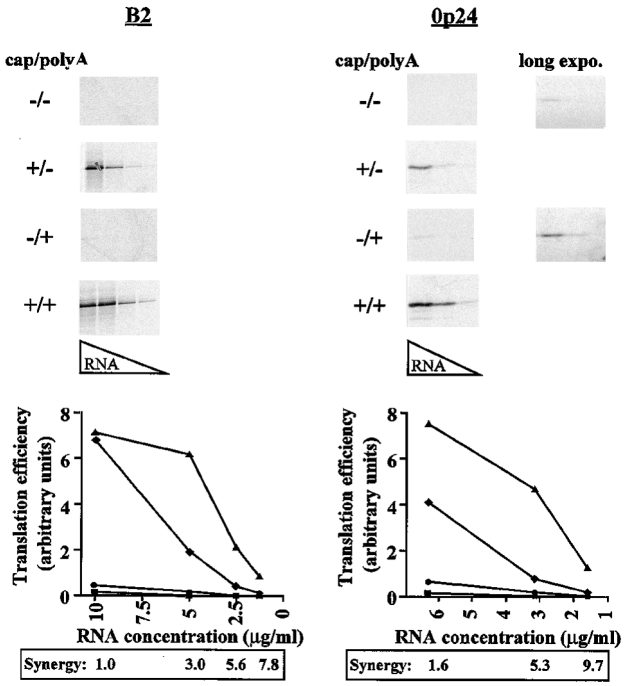

FIG. 4. **Sensitivity of cap-poly(A) synergy to RNA concentration in ribosome-depleted RRL.** Ribosome-depleted RRL was programmed with different final concentrations of mRNAs derived either from pB2 (*left-hand side*) or from p0p24 (*right-hand side*) transcribed in the form indicated alongside each panel. Final RNA concentrations were 10, 5, 2.5, or 1.25 μg/ml for B2 mRNAs and 6.3, 3.15, or 1.575 μg/ml for 0p24 mRNAs. Translation products were analyzed as described in the legend to Fig. 2. For reactions programmed with −/− and −/+ 0p24 mRNAs, a second panel is shown that corresponds to an 8-fold overexposure of the gel (*long expo. panels*). The translation efficiencies of the various RNAs (*squares,* −/−; *circles,* −/+; *diamonds,* +/−; and *triangles,* +/+) plotted as a function of RNA concentration and the cap-poly(A) synergy calculated at each RNA concentration are shown *below* the two series of panels.

proportions of 40 S and 60 S ribosomal subunits present in the different translation systems used (Fig. 2*B*). The concentration of 60 S and 40 S ribosomal subunits in ribosome-depleted RRL was below the detection limit of the assay (middle plot), whereas, compared with RRL (*upper plot*), larger 40 S and 60 S peaks and an additional peak corresponding to 80 S ribosomes could be detected in RRL supplemented with non-nucleased HeLa cell extract (*lower plot*). As an additional control of the ribosome-depleted system, it was verified that ultracentrifugation had not irreversibly altered the nature of the translation extracts. Indeed, back-addition of the ribosomes pelleted during ultracentrifugation totally restored translation activity to levels observed in control RRL (Fig. 2*C* and data not shown). More importantly, cap-poly(A) synergy was reduced when 0.8× ribosomes (with respect to starting extract) were included in the reaction and was abolished when 1.6× ribosomes were added back.

Examination of Cap and Poly(A) Cooperativity in Human Cell-free Extracts—We next examined whether a similar strategy for inducing poly(A) dependence could be used with other cell-free extracts. Similarly to standard RRL, only a minor translational advantage is conferred upon polyadenylation of a capped B2 RNA in a nuclease-treated translation-competent HeLa S10 extract (Fig. 3*A, 2 left-hand lanes*). When HeLa cell extracts were submitted to ultracentrifugation, supernatants were totally lacking in translation activity (Fig. 5*A, 0*× *lanes*) unless they were supplemented with a fraction of the ribosomes recovered from the ultracentrifugation pellet (Fig. 3*A, 0.3* and *0.6*× *lanes*). Sucrose gradient analysis, performed to control extract composition, confirmed the significantly reduced concentrations of free 40 S and 60 S ribosomal subunits in the depleted extracts (Fig. 3*A*). In depleted extracts reconstituted with 0.3× ribosomes, polyadenylation increased translation efficiency of a capped mRNA 3–4-fold. Moreover, a modest cap-poly(A) synergy was observed (approximately 2.5-fold, see Fig. 3*B*), demonstrating that the ability to render extracts poly(A)-dependent by ultracentrifugation is not a peculiarity of the RRL system.

Synergy in Ribosome-depleted RRL Is Sensitive to mRNA Concentration—The levels of synergy reported above in ribosome-depleted RRL (2–3-fold) were rather modest when compared with those observed from *in vivo* studies (see for example Ref. 9). In an attempt to increase synergy in the RRL system, we first optimized the concentrations of added KCl and $MgCl_2$ with respect to +/+ mRNA translation (data not shown; optima of 115 and 0.9 mM respectively, as opposed to 102 and 0.8 mM used for the experiments shown in Fig. 2) and then examined the effects of RNA concentration on synergy. A second series of mRNAs transcribed from p0p24 cDNAs (Fig. 1) was included in the analysis to show that the effects observed so far were not an artifact of the pB2 constructs. Whereas the B2 and 0p24 RNAs share an identical 150-nt 3′-UTR/poly(A) tract, the cyclin B2 5′-UTR and coding region in the 0p24 mRNAs are replaced by a short oligonucleotide-derived 5′-UTR preceding the HIV-I p24-coding region.

B2 and 0p24 mRNAs were thus used to program ribosome-depleted RRL translation reactions at a range of final RNA concentrations, and the degree of cap-poly(A) synergy was calculated at each concentration (Fig. 4). Similar levels of synergy

were observed with equivalent molar concentrations of the 0p24 and B2 mRNAs (950 and 1450 nt long, respectively), indicating that cap-poly(A) cooperativity is likely to be a general phenomenon on mRNAs translated in this system. It should be noted that kinetic experiments failed to detect any differences in the functional half-lives between RNAs that were capped, polyadenylated, or both (data not shown), even when extremely low concentrations of programming RNA were used. Thus, synergy does not result from significant differences in mRNA stability in these extracts. More important, although virtually no synergy was evidenced with near-saturating concentrations of the B2 and 0p24 mRNAs, synergy increased significantly as the RNA concentration was reduced and reached almost 8- and 10-fold, respectively, at the lowest concentrations tested. This increase in observed synergy stemmed from the extremely inefficient translation of the +/− RNAs at all but the highest RNA concentrations. Indeed, in all such experiments, the dose responses for +/− mRNAs showed significant non-linearity at the lower end of the RNA concentration range (see also for example Fig. 7). It is plausible that this non-linearity reflects the inability of the +/− mRNAs to compete with the endogenous RNA fragments generated by nuclease treatment of the lysate. It is also interesting that synergy is highest when low RNA concentrations are used to program ribosome-depleted RRL, whereas no synergy is observed in standard RRL at any RNA concentration (Fig. 2, and data not shown). Although we have no concrete explanation for this discrepancy, these data imply that the factors that are limiting in ribosome-depleted RRL are never limiting in standard RRL. In the light of the data presented above, subsequent translation experiments in depleted RRL were performed with optimal KCl and $MgCl_2$ concentrations and a compromise of mRNAs concentrations that allow significant synergy while yielding easily detectable amounts of translation products.

The PABP-eIF4G Interaction Mediates the Translational Effects of the Poly(A) Tail—To characterize the molecular requirements for cap-poly(A) synergy in the RRL-based system, we employed the group A rotavirus NSP3 protein. In addition to binding specifically a conserved sequence present at the 3′ end of all rotaviral mRNAs (15), NSP3 was recently shown to interact directly with the N-terminal part of eIF4G and, in doing so, to evict PABP from the eIF4F complex (16). Thus, if cap-poly(A) synergy depends on mRNA circularization mediated by the eIF4G-PABP interaction, it should be abolished by NSP3. For the study presented here, a truncated form of recombinant NSP3 spanning amino acids 163–313 was used. This fragment is deleted for the rotaviral RNA binding domain but is still capable of disrupting the eIF4G-PABP interaction (16, 21).

First, the effects of NSP3 on the translation of a pool of cellular mRNAs were determined, by including pure protein in standard RRL reactions containing non-nucleased HeLa cell S10 extract as a source of mRNAs. NSP3 significantly inhibited global protein synthesis in a dose-dependent manner, with inhibition attaining over 70% when NSP3 concentrations exceeded 12 μg/ml (Fig. 5*A*). It was confirmed that the recombinant NSP3 fragment was displacing PABP from the eIF4F complex in this system by immunoprecipitating the eIF4F complex with antibodies directed against eIF4G, and analyzing the immunocomplexes by Western blotting with antibodies raised against PABP (Fig. 5*B*). Inclusion of NSP3 in translation reactions dramatically reduced the quantity of PABP which co-immunoprecipitated with eIF4G. These data, together with results of similar experiments performed with rotavirus-infected cell extracts (16), demonstrate that in the absence of the eIF4G-PABP interaction the RNA-protein interactions alone are not sufficiently stable to withstand the precipitation conditions. This is possibly because the affinities of the separated proteins for mRNA ends are lower than those of the intact eIF4G·PABP complex (see "Discussion"). Interestingly, even with high concentrations of added NSP3, PABP eviction from eIF4G was not complete. Effectively, co-immunoprecipitation of PABP with eIF4G from translation reactions containing 50 μg/ml of added NSP3 approached 20% of that observed in reactions without NSP3. This is the first direct demonstration that NSP3 can inhibit translation of cellular mRNAs, presumably via its interaction with eIF4G and displacement of PABP.

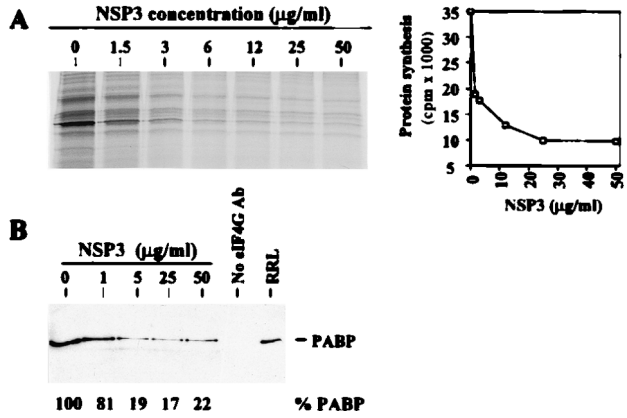

FIG. 5. **NSP3 evicts PABP from eIF4G and inhibits endogenous mRNA translation.** *A,* standard RRL reactions were programmed with the endogenous mRNAs present in non-nucleased HeLa cell S10 extract (33% v/v S10 extract) and received recombinant truncated rotavirus NSP3 protein in H100 buffer (concentrations in μg/ml, indicated *above* each lane) or H100 buffer alone (*0 lane*). The exposure shown is 8-fold longer than when *in vitro* transcribed RNAs were analyzed. Alongside is plotted the radioactivity incorporated into proteins as determined by trichloroacetic acid precipitation. *B,* translation reactions (150 μl) were assembled as described in *A* in the presence of the indicated concentrations of NSP3, prior to immunoprecipitation with antibody against eIF4G and Western blotting with antibodies (*Ab*) against PABP (see "Experimental Procedures"). A control reaction contained no anti-eIF4G antibody. RRL (0.25 μl) was loaded alongside to serve as a marker for the position of endogenous PABP (*RRL lane*). The percentage of PABP in the immunoprecipitate is indicated *below* each lane (100% is the value obtained in the absence of NSP3).

Next, the effect of NSP3 on each of the four different forms of *in vitro* transcribed B2 and 0p24 mRNAs was examined in standard and ribosome-depleted RRL (Fig. 6). The final concentration of NSP3 used (5 μg/ml) corresponds to the minimal concentration required to reduce translation of cellular mRNAs by 50% and to displace 80% of PABP from the eIF4F complex (see Fig. 5). NSP3 had no significant effect on the translation efficiency of the non-polyadenylated RNAs in either translation system (Fig. 6, *A* and *B*, see −/− and +/− *lanes*). In contrast, NSP3 reduced the translation efficiency of each capped polyadenylated RNA to approach that of its non-polyadenylated counterpart in ribosome-depleted RRL (Fig. 6, *A* and *B*, +/+ and +/− *lanes*), severely diminishing cap-poly(A) synergy. These results strongly suggest that synergy requires mRNA circularization mediated by the eIF4G-PABP interaction. Interestingly, NSP3 inclusion in standard RRL reactions reduced the translation efficiency of polyadenylated RNAs to approach that of their non-polyadenylated equivalents, irrespective of the mRNA cap status. These data imply that poly(A) tail-mediated stimulation of translation in standard RRL also requires the PABP-eIF4G interaction. This hypothesis is indirectly supported by results obtained using the human rhinovirus 2A proteinase, which cleaves eIF4G such that its PABP/eIF4E-binding domain is separated from the region that fixes the ribosome-associated eIF3 complex (13, 20, 30). Not only did this proteinase dramatically inhibit translation of capped B2 RNAs in either system, it also showed the same

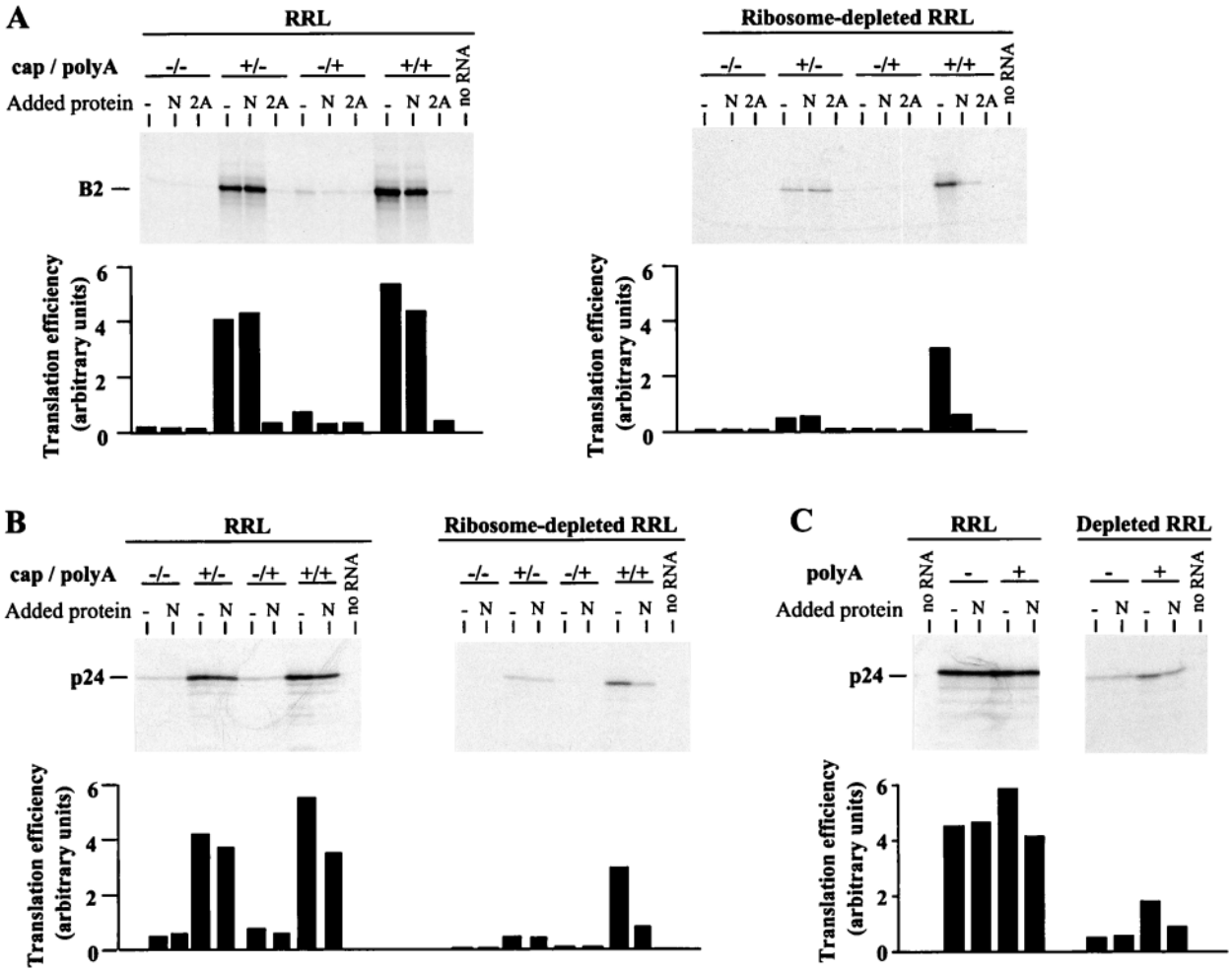

FIG. 6. **Cap-poly(A) synergy requires the interaction between PABP and eIF4G.** Standard or ribosome-depleted RRL was programmed with B2 (*A*), 0p24 (*B*), or EMCVp24 (*C*) mRNAs. Final RNA concentrations were 3 μg/ml (for 0p24 mRNAs) and 6.2 μg/ml (for EMCVp24 mRNAs), and for B2 mRNAs were 2.6 μg/ml (in ribosome-depleted RRL) or 6.5 μg/ml in standard RRL (to facilitate the detection of B2 translation products in RRL reactions treated with 2A proteinase). Reactions were supplemented with H100 buffer (*– lanes*), recombinant truncated NSP3 protein (5 μg/ml; *N lanes*), or rhinovirus 2A proteinase (10 μg/ml; *2A lanes*) each in H100 buffer. Translation products were analyzed as described in the legend to Fig. 2. Calculated cap-poly(A) synergies for the B2 and 0p24 mRNAs in ribosome-depleted RRL were, respectively, 5.1- and 5.9-fold in the absence of NSP3, as compared with 1.3- and 1.8-fold in the presence of NSP3. Poly(A)-mediated stimulation of EMCVp24 was 3.7-fold in the absence and 1.8-fold in the presence of NSP3. In three independent experiments, poly(A) stimulation of EMCV IRES-driven translation in depleted RRL was 3-, 3.7-, and 4.5-fold.

effects as NSP3 on translation of uncapped polyadenylated B2 RNA in RRL, *i.e.* the efficiency was reduced to approach that of uncapped non-polyadenylated RNA (Fig. 6*A, 2A lanes*).

The standard RRL system is often used to study the translation of non-classical IRES-containing mRNAs. We evaluated whether one such IRES, that of encephalomyocarditis virus (EMCV, a picornavirus), would still be translationally active in the ribosome-depleted RRL system. The full EMCV IRES was inserted into the oligonucleotide linker of p0p24 such that p24 synthesis will be driven from the authentic viral AUG at the 3′ end of the IRES (Fig. 1). Since picornaviral RNAs are naturally uncapped, only two versions of the EMCVp24 RNA were generated, differing in the presence or absence of the 3′ poly(A) tail. The corresponding transcripts were translated in either standard or ribosome-depleted RRL, with and without 5 μg/ml of added NSP3 (Fig. 6*C*). The efficiency of EMCVp24 translation was significantly reduced in ribosome-depleted as compared with standard RRL (Fig. 6*C*). However, we consider that the EMCV IRES was still functional in the depleted extract since the uncapped, non-polyadenylated version of this RNA was translated some 15-fold better than the equivalent −/− 0p24 mRNA (Fig. 6). In addition, the EMCV IRES is still functional in ribosome-depleted RRL when inserted between the two cistrons of a dicistronic mRNA, confirming that it is behaving as an IRES (data not shown).

Polyadenylation of the uncapped EMCVp24 mRNA reproducibly stimulated translation 3–4-fold in the ribosome-depleted extract, whereas it had only a slight positive effect on IRES activity in standard RRL reactions. Inclusion of NSP3 in the reactions abolished the modest poly(A)-mediated stimulation of translation driven from the EMCV IRES in RRL and also significantly reduced the stimulation seen in ribosome-depleted RRL (Fig. 6*C, N lanes*), demonstrating that the eIF4G-PABP interaction is required for maximal poly(A)-mediated stimulation of translation on this uncapped, IRES-containing mRNA.

Cap-Poly(A) Synergy Is Not Affected by Increasing the Distance between the Open Reading Frame and the Poly(A) Tail— One possible result of circularization of mRNAs with relatively short 3′-UTRs is that terminating ribosomes are in the proximity of the mRNA 5′ end, which could serve to facilitate recycling of ribosomal subunits from the mRNA 3′ end back to the 5′ cap (for reviews see Refs. 3 and 31). Thus, we investigated the impact of the length of the mRNA that separates the end of the open reading frame from the poly(A) tail on cap-poly(A) cooperativity. Toward this end, a dicistronic mRNA transcribed from pB20p24 (see Fig. 1) was generated, which

has the same 5′ and 3′-UTRs as the monocistronic B2 mRNA, but carries a second translatable cistron encoding the HIV-I p24 protein preceded by a short polylinker. This could be used to determine whether ribosome arrival near the mRNA 3′ end is required for cap-poly(A) synergy, since the RRL translation system is inefficient in reinitiating translation of downstream cistrons in polycistronic messages. However, since it is formally possible that ribosomes could scan past the start site of the second cistron without re-initiating translation, a cDNA was constructed such that dicistronic RNAs would contain a truncated, inactive IRES from human rhinovirus type 2 between the two cistrons (Fig. 1, *pB2ΔIRESp24*). We have previously demonstrated that this inactive IRES presents a barrier to ribosomal scanning and downstream cistron translation without competing significantly with the upstream cistron for translation components (18).

RNAs with the four different combinations of cap and/or poly(A) tail were transcribed from these different cDNAs and used to program ribosome-depleted RRL translation reactions at a range of molar equivalent RNA concentrations. No p24 synthesis could be evidenced in reactions programmed with the dicistronic B20p24 or B2ΔIRESp24 RNAs, confirming the absence of reinitiation and downstream cistron translation in the ribosome-depleted extracts (Fig. 7). Of more interest, the B2 cistron of the B2, B20p24, and B2ΔIRESp24 RNAs was translated with very similar efficiency in the three cases, and the three mRNAs behaved almost identically with respect to the cooperative effects of the cap and poly(A) tail at the different mRNA concentrations. These results infer that cap-poly(A) cooperativity is insensitive to increasing the distance that separates the termination codon and the poly(A) tail and that there is no advantage for a capped-polyadenylated RNA if ribosomes terminate translation 150 nt (on B2 RNA) rather than 1200 nt (in the case of the B2ΔIRESp24 RNA) upstream of the mRNA 3′ end.

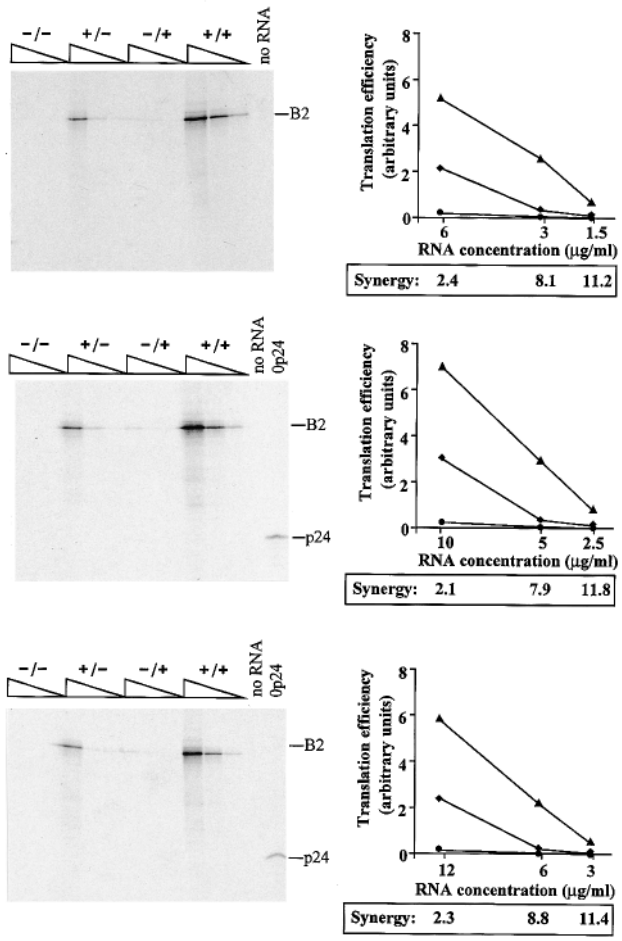

FIG. 7. **Cap-poly(A) synergy is not quantitatively affected on dicistronic mRNAs with downstream silent open reading frames.** Ribosome-depleted RRL extracts were programmed with equivalent molar concentrations of B2, B20p24, or B2ΔIRESp24 mRNAs as described in the legend to Fig. 4 (RNA concentrations in μg/ml: 6.2, 3.1, and 1.55 for B2; 10, 5.0, and 2.5 for B20p24; and 12.5, 6.25, and 3.125 for B2ΔIRESp24). A control reaction was programmed with water (*no RNA lane*). A reaction programmed with 0p24 mRNA was loaded alongside to indicate the position of the p24 gene product (*0p24 lane*). Presentation of the data is exactly as in the legend to Fig. 4. Curves for −/− mRNAs were omitted for clarity.

DISCUSSION

To our knowledge, the translation systems described here are the first mammalian *in vitro* extracts that support cap-poly(A) synergistic stimulation of translation in the absence of intact competitor RNAs. RRL extracts were rendered poly(A)-dependent by partial depletion of ribosomal subunits, and presumably their tightly associated translation factors, via ultracentrifugation. Control experiments based on high salt treatment of cell extracts before ultracentrifugation suggest that reduced concentrations of both ribosomes and initiation factors contribute to synergy.[2] However, it cannot be ruled out that ultracentrifugation also serves to remove certain general RNA-binding proteins that could reduce the effects of the mRNA poly(A) tail on translation in non-depleted extracts. Under optimal conditions, the ribosome-depleted RRL extracts exhibited levels of synergy (8–10-fold) comparable to those reported for *Drosophila* embryo and yeast cell-free extracts (synergies of 3–15-fold depending on the system), in which mRNA competition was used to confer poly(A) dependence (6, 8, 10, 28). It should be noted that global translation efficiency of *in vitro* transcribed mRNAs was significantly lower in ribosome-depleted as opposed to intact RRL. We believe that this is not a major concern, since, when compared with the highly competitive environment of the intact cell, standard RRL exhibits extremely elevated translation levels for a given RNA species. Translation-competent HeLa cell S10 extracts could also be rendered moderately poly(A)-dependent (synergy of 2.5-fold) by ultracentrifugation. However, due to the intrinsically lower translation activity of HeLa cell extracts in our hands as compared with RRL, it was difficult to reproducibly improve synergy by reducing mRNA concentration (data not shown).

The ability to generate poly(A)-dependent extracts without intact competitor RNA addition allowed us to address the question of mRNA circularization as the molecular basis of cap-poly(A) cooperativity. We used the rotaviral NSP3 protein to interrupt the PABP-eIF4G interaction invoked in the closed loop model of translation initiation. To date, this is the only known initiation factor complex affected by NSP3, although it cannot be formally excluded that other protein-protein interactions are also sensitive to the rotaviral protein. Cap-poly(A) synergy in poly(A)-dependent extracts was severely reduced (although not completely abolished) by NSP3, demonstrating that the PABP-eIF4G interaction is required for maximal synergy. In favor of the hypothesis that cap-poly(A) cooperativity relies on eIF4F/PABP-mediated mRNA circularization, it has been reported that the interaction of wheat germ PABP with eIF4F increases the affinity of eIF4E for cap analogue by some 40-fold, and conversely that the affinity of eIF4F-complexed plant PABP for poly(A) is greater than that of free PABP (32, 33). It also seems plausible from our data that the additive effects of capping and polyadenylation in standard RRL result

[2] Borman, A. M., Michel, Y. M., and Kean, K. M. (2000) *Nucleic Acids Res.*, in press.

from mRNA circularization, since they were abolished by NSP3. However, the translational advantage conferred by circularization in this case is minimal, presumably because ribosomes and associated translation factors are not limiting.

The poly(A) tail also moderately stimulated translation initiation on uncapped RNAs, in accordance with previous reports (6, 8). However, compared with control RRL, this stimulation was reduced when extracts were partially depleted of ribosomes. Interestingly, the poly(A)-mediated stimulation of uncapped RNA translation also requires intact eIF4G complexed to PABP, as indicated by sensitivity to the NSP3 and 2A proteins (see Fig. 6). These results are in agreement with those of Ref. 28, where eIF4G mutations were used to interrupt the eIF4G-PABP interaction in yeast. It is possible that the eIF4G·PABP complex also induces circularization of uncapped-polyadenylated RNAs. However, it remains to be determined whether eIF4G complexed to PABP can bind RNA directly, for instance via its RNA recognition motif (2, 34).

Another aspect of the experiments reported here concerns the general inhibition of *in vitro* translation of a pool of cellular mRNAs by purified recombinant rotaviral NSP3 protein. Once again, the known physiological properties of NSP3 support the concept that actively translated cellular mRNAs are circularized via a cap-eIF4E-eIF4G-PABP-poly(A) interaction. Furthermore, these data constitute the first direct evidence that NSP3 alone is sufficient to provoke the shut-off of host cell translation seen during rotavirus infection. Inhibition of *in vitro* translation of endogenous mRNAs by recombinant NSP3 reproducibly reached a plateau at around 70% inhibition. The residual translation reflected a global inefficient translation of mRNAs within the pool rather than continued translation of a specific subpopulation of mRNAs, and thus probably corresponds to the efficiency of "poly(A)-independent" translation in this system. However, NSP3-induced displacement of PABP from eIF4G was not total and reached a plateau at around 80% displacement (see Fig. 5). The subpopulation of the eIF4F-PABP complex that resists NSP3 might be partly responsible for the residual translation observed with endogenous mRNAs in NSP3-treated extracts (Fig. 5*A*). Similarly, it could explain why NSP3 did not totally abolish cap-poly(A) synergy (Fig. 6). Further studies will be required to dissect the nature of this apparently NSP3-resistant proportion of the eIF4F·PABP complex.

We have also shown that the introduction of a barrier to 40 S ribosomal scanning followed by a second, non-translated open reading frame between the reporter gene and the poly(A) tail does not quantitatively affect translation efficiency or cap-poly(A) cooperativity. These data imply that the length of the effective 3′-UTR is of little importance to mRNA 5′-3′ end interplay, which is directly relevant to the many natural mRNAs that have extremely long 3′-UTRs containing silent open reading frames. In addition, these data argue against the simplistic hypothesis that synergy results from post-termination 40 S ribosomal subunits reaching the poly(A) tail and then being directly transferred back to the 5′ cap. Instead one might speculate that, if ribosome recycling occurs, it is either indirect preferential re-recruitment of dissociated ribosomal subunits that remain in the proximity of the "donor" mRNA or direct recycling from the vicinity of the termination codon. In this respect, it is interesting to note that PABP was recently shown to interact with a component of the eukaryotic translation termination machinery (35). To resolve completely the mechanism resulting in synergy, it would be advantageous to determine whether an RNA behaves "catalytically" or "stoichiometrically" in the depleted extract. Unfortunately, from the data presented here, it is difficult to discriminate convincingly between these two types of behavior. The dose responses of the different mRNAs translated in depleted extract all exhibit some non-linearity, which could be interpreted as indicative of catalytic action. However, as we have already pointed out (see "Results," this non-linearity could equally reflect competition between the added transcripts and fragments of endogenous mRNA generated by micrococcal nuclease treatment of the translation extracts. Further studies will be required to address fully this question.

Finally, we demonstrated that the effects of polyadenylation on non-classical, IRES-containing mRNAs can be studied in these systems. EMCV IRES-driven translation was stimulated severalfold by addition of a poly(A) tail to the uncapped IRES-carrying mRNA, an effect that was diminished by NSP3. These results suggest that the mechanism of 5′–3′ end cross-talk operative on classical cellular mRNAs is at least partly conserved for certain IRES-containing messages. We are currently evaluating the effects of polyadenylation on the IRES activities of other members of the picornavirus family, many of whom are known to induce the cleavage of PABP and/or eIF4G during infection of the host cell.

Acknowledgments—We acknowledge the skillful technical assistance of N. Castagné. We also thank Sylvie van der Werf and Cécile Malnou for their interest in this work. Work in the laboratory of K. M. K. was supported by the Program de Recherche Clinique de l'Institut Pasteur and by Grant 6495 from the Association Française Contre les Myopathies.

REFERENCES

1. Banerjee, A. K. (1980) *Microbiol. Rev.* **44,** 175–205
2. Morley, S. J., Curtis, P. S., and Pain, V. M. (1997) *RNA* (*NY*) **3,** 1085–1104
3. Jacobson, A. (1996) in *Translational Control* (Hershey, J. W. B., Mathews, M. B., and Sonenberg, N., eds) pp. 451–480, Cold Spring Harbor Laboratory, Cold Spring Harbor, New York
4. Doel, M. T., and Carey, N. H. (1976) *Cell* **8,** 51–58
5. Tarun, S. Z., Jr., and Sachs, A. B. (1995) *Genes Dev.* **9,** 2997–3007
6. Preiss, T., and Hentze, M. W. (1998) *Nature* **392,** 516–520
7. Munroe, D., and Jacobson, A. (1990) *Mol. Cell. Biol.* **10,** 3441–3455
8. Iizuka, N., Najita, L., Franzusoff, A., and Sarnow, P. (1994) *Mol. Cell. Biol.* **14,** 7322–7330
9. Gallie, D. R. (1991) *Genes Dev.* **5,** 2108–2116
10. Gebauer, F., Corona, D. F. V., Preiss, T., Becker, P. B., and Hentze, M. W. (1999) *EMBO J.* **18,** 6146–6154
11. Proweller, A., and Butler, S. (1997) *J. Biol. Chem.* **272,** 6004–6010
12. Tarun, S. Z., Jr., and Sachs, A. B. (1996) *EMBO J.* **15,** 7168–7177
13. Imataka, H., Gradi, A., and Sonenberg, N. (1998) *EMBO J.* **17,** 7480–7489
14. Wells, S. E., Hillner, P. E., Vale, R. D., and Sachs, A. B. (1998) *Mol. Cell* **2,** 135–140
15. Poncet, D., Aponte, C., and Cohen, J. (1993) *J. Virol.* **67,** 3159–3165
16. Piron, M., Vende, P., Cohen, J., and Poncet, D. (1998) *EMBO J.* **17,** 5811–5821
17. Jackson, R. J., Hunt, S. L., Gibbs, C. L., and Kaminski, A. (1994) *Mol. Biol. Rep.* **19,** 147–159
18. Borman, A., and Jackson, R. J. (1992) *Virology* **188,** 685–696
19. Wain-Hobson, S., Sonigo, P., Danos, O., Cole, S., and Alizon, M. (1985) *Cell* **40,** 9–17
20. Liebig, H.-D., Ziegler, E., Yan, R., Hartmuth, K., Klump, H., Kowalski, H., Blaas, D., Sommergruber, W., Frasel, L., Lamphear, B., Rhoads, R. E., Kuechler, E., and Skern, T. (1993) *Biochemistry* **32,** 7581–7588
21. Piron, M., Delaunay, T., Grosclaude, J., and Poncet, D. (1999) *J. Virol.* **73,** 5411–5421
22. Borman, A., Howell, M. T., Patton, J., and Jackson, R. J. (1993) *J. Gen. Virol.* **74,** 1775–1788
23. Molla, A., Paul, A. V., and Wimmer, E. (1991) *Science* **254,** 1647–1651
24. Borman, A. M., Kirchweger, R., Zeigler, E., Rhoads, R. E., Skern, T., and Kean, K. M. (1997) *RNA* (*NY*) **3,** 186–196
25. Dasso, M. C., and Jackson, R. J. (1989) *Nucleic Acids Res.* **17,** 6485–6497
26. Jackson, R. J., and Hunt, T. (1983) *Methods Enzymol.* **96,** 50–74
27. Foiani, M., Cigan, A. M., Paddon, C. J., Harashima, S., and Hinnebusch, A. G. (1991) *Mol. Cell. Biol.* **11,** 3203–3216
28. Tarun, S. Z., Jr., Wells, S. E., Deardorff, J. A., and Sachs, A. B. (1997) *Proc. Natl. Acad. Sci. U. S. A.* **94,** 9046–9051
29. Preiss, T., Muckenthaler, M., and Hentze, M. W. (1998) *RNA* (*NY*) **4,** 1321–1331
30. Lamphear, B. J., Kirchweger, R., Skern, T., and Rhoads, R. E. (1995) *J. Biol. Chem.* **270,** 21975–21983
31. Gallie, D. R. (1998) *Gene* (*Amst.*) **216,** 1–11
32. Le, H., Tanguay, R. L., Balasta, M. L., Wei, C. C., Browning, K. S., Metz, A. M., Goss, D. J., and Gallie, D. R. (1997) *J. Biol. Chem.* **272,** 16247–16255
33. Wei, C.-C., Balasta, M. L., Ren, J., and Goss, D. J. (1998) *Biochemistry* **37,** 1910–1916
34. de Gregorio, E., Preiss, T., and Hentze, M. W. (1998) *RNA* (*NY*) **4,** 828–836
35. Hoshino, S., Imai, M., Kobayashi, T., Uchida, N., and Katada, T. (1999) *J. Biol. Chem.* **274,** 16677–16680